Journal of Molecular and Engineering Materials
Vol. 3, Nos. 1 & 2 (2015) 1540008 (7 pages)

DOI: 10.1142/S2251237315400080

World Scientific
www.worldscientific.com

Competitive Self-Assembly Manifests Supramolecular Darwinism in Soft-Oxometalates

Santu Das, Saurabh Kumar, Apabrita Mallick and Soumyajit Roy*
Eco-Friendly Applied Materials Laboratory (EFAML)
Materials Science Centre, Department of Chemistry
Indian Institute of Science Education and Research Kolkata
Mohanpur – 741246, India
**s.roy@iiserkol.ac.in*

Received 2 August 2015
Accepted 8 September 2015
Published 25 September 2015

Topological transformation manifested in inorganic materials shows manifold possibilities. In our present work, we show a clear topological transformation in a soft-oxometalate (SOM) system which was formed from its polyoxometalate (POM) precursor [PMo_{12}@$Mo_{72}Fe_{30}$]. This topological transformation was observed due to time dependent competitive self-assembly of two different length scale soft-oxometalate moieties formed from this two-component host–guest reaction. We characterized different morphologies by scanning electron microscopy, electron dispersive scattering spectroscopy, dynamic light scattering, horizontal attenuated total reflection–infrared spectroscopy and Raman spectroscopy. The predominant structure is selected by its size in a sort of supramolecular Darwinian competition in this process and is described here.

Keywords: Polyoxometalate; soft-oxometalate; topological transformation; competitive self-assembly.

1. Introduction

Hierarchical self-assembly of molecular metal-oxide based structures has been achieved using chemical and symmetry principles.[1–5] Exploitation of chemical principles (redox cascade, for instance) has led to the formation of unusual icosahedral isopoly and heteropolyoxometalate clusters.[6–23] Transcending the molecular frontier in supramolecular regime, further assembly has been achieved by the operation of a length-scale and symmetry controlled supramolecular Darwinian principle,[24] where the larger and more symmetric species is selected, for instance, the assembly of [$PMo_{12}O_{40}$@$Mo_{72}Fe_{30}$].[25] Here starting from a relatively small sized $PMo_{12}O_{40}$ precursor in the presence of Fe^{3+}, the more symmetric and rather large $Mo_{72}Fe_{30}$ cluster is formed depleting the starting precursor whereas the starting PMo_{12} gets encapsulated in the larger and more symmetric $Mo_{72}Fe_{30}$. It has been shown by us and others that each of the components of the above host–guest species [PMo_{12}@$Mo_{72}Fe_{30}$] i.e., PMo_{12} and $Mo_{72}Fe_{30}$ independently shows superstructured soft-oxometalate (SOM) formation by spontaneous assembly in colloidal length-scales.[1,2,26–43] We have previously shown that a dilute sonicated dispersion of PMo_{12} leads to the

*Corresponding author.

formation of peapod[37] like SOM structures. Initially, the peapods have nanosphere-type morphology and with time these spheres get converted to nanorods with nanospheres embedded inside this rod. The length and the diameter of these rods are found to be around 2 μm and 500 nm, respectively. In acidic pH, the spherical seeds from the peapods leech out and the peapods are converted to rod shaped structures. Likewise, $Mo_{72}Fe_{30}$ dispersion showed spontaneous macro ionic blackberry[27]-like SOM assembly where $Mo_{72}Fe_{30}$ slowly formed super structure in dispersion. Initially, the presence of both single molecule $Mo_{72}Fe_{30}$-based SOM superstructure as well as self-assembled $Mo_{72}Fe_{30}$ in dispersion was observed. With time, concentration of single molecule decreased and self-assembled structure increased which confirmed the increasing hydrodynamic radius of self-assembled $Mo_{72}Fe_{30}$. Further, it was also shown that the hydrodynamic radius of hollow vesicle decreased with increasing pH of the solution. With these trends in mind we ask what happens if we induce these two self-assembly processes simultaneously? Will these self-assembly processes be co-operative or would they be competitive and manifest supramolecular Darwinian principles in operation? To do so, we started with a dilute preformed $[PMo_{12}O_{40}@Mo_{72}Fe_{30}]$ cluster's dispersion and monitored its time dependent evolution in colloidal length-scales. We first describe the experimental details of this system.

2. Experimental Procedure

2.1. *Materials and reagents*

All the materials were purchased from commercially available sources and used without further purification. All the glasswares were first boiled in acid bath, then washed with water and finally cleaned with acetone. They were properly dried in hot air oven over-night. We used doubly distilled deionized water in all the experiments.

2.2. *Preparation of* $[PMo_{12}O_{40}@Mo_{72}Fe_{30}]$

This precursor POM was prepared according to literature method.[25] Yellow palette like crystals were obtained after one week. Yellow crystals were filtered off and dried in vacuum for 12 h.

2.3. *Preparation of* $[PMo_{12}O_{40}@Mo_{72}Fe_{30}]$*-based SOM*

10 mg of POM was added to 4 mL of double-distilled water and then sonicated for 10 min. After that, this mixture was heated to 80°C in a silicon oil bath and finally cooled at 0°C for 10 min in a refrigerator. A yellow dispersion of POM was formed which is referred to as SOM here.

2.4. *Observation of different morphology at different time intervals*

In a clean dried vial, 4 mL of SOM was taken and kept at room temperature and in open air for several hours. After each hour time interval, we prepared SEM samples from the dispersion and monitored the morphology of the samples at these time intervals.

2.5. *Characterizations*

2.5.1. *Sample preparation for taking SEM image and EDS analysis*

SOM was diluted further and then drop casted on a silicon wafer and dried in normal aerobic condition for 2 days and further dried in vacuum for 24 h before doing the experiment. SEM and EDS experiments were done using SUPRA 55 VP-41-32 instrument with the SmartSEM version 5.05 Zeiss software and EDS Oxfored software.

2.5.2. *Horizontal attenuated total reflectance-infrared spectroscopy*

Diluted dispersion of SOM was put on a zinc selenide plate which was separately attached with FT-IR machine for measuring IR spectrum in water. Perkin Elmer Spectrum RX1 spectrophotometer with horizontal attenuated total reflectance (HATR) facility in the range 2500–400 cm^{-1} was used to record HATR-IR spectra.

2.5.3. *Raman spectroscopy*

Diluted dispersion of SOM was taken in a fluorescence glass cuvette with square aperture and Raman spectroscopy was performed within the range of 300–1200 cm^{-1} with an excitation wave length of 633 nm.

2.5.4. *Dynamic light scattering measurement*

Average size of the particle was obtained using dynamic light scattering method in a Malvern Zetasizer instrument. A very dilute solution of SOM was prepared by further dilution of the SOM dispersion and taking it in a fluorescence glass cuvette with square aperture and the instrument was set to take 15 runs before measuring the average hydrodynamic radius of the SOM.

3. Result and Discussion

3.1. *Time dependent topological transformation*

$[PMo_{12}O_{40}@Mo_{72}Fe_{30}]$ was dispersed in water by sonication and heating. This dispersion was kept at room temperature under normal conditions. At different time intervals, we monitored the SEM images of the dispersion by drop casting the dispersion on silicon wafer and we observed that there is speciation in the dispersion (Fig. 1). From the SEM investigation, it is observed that initially nanospheres are formed [Fig. 1(a)]. They remain spherical up to 3 h. Beyond 3 h, the shape changes from nanosphere to nanorods [Fig. 1(b)] i.e., there is a conversion of more symmetric topology to less symmetric topology. Mathematically, such topological transformation can be achieved by removal of 12 C_5-axis from the sphere and introducing a C_∞-axis (Fig. 1). Time scale for such topological transformation induced by sonication and heating on the precursor structure vary significantly between the host $Mo_{72}Fe_{30}$ and the guest $PMo_{12}O_{40}$ moieties. Now we address a question: what are the length scales of the SOMs formed from the precursor host and guest moieties? The size of the SOM formed from the host moiety is around 200 nm and for that formed from guest moiety is few micrometers in the dispersion when we make separate dispersions of the host and guest precursors. In our present precursor, $PMo_{12}O_{40}$ is encapsulated inside $Mo_{72}Fe_{30}$. With sonication, the dimensions of self-assembled SOM formed from ($PMo_{12}O_{40}$) is larger than the SOM formed from the host ($Mo_{72}Fe_{30}$). The guest species SOM-peapod thus disrupts hollow vesicles of $Mo_{72}Fe_{30}$ due to competitive self-assembly where SOM length scale or size determines which component plays the dominant role in deciding the overall topology of the species in the dispersion following a sort of Supramolecular Darwinian selection.[24] Therefore, we observed nanorods as time evolved in the dispersion [Fig. 1(b)]. Here the selection is based only on the size. Larger SOM-peapods from $[PMo_{12}]$ dominate over smaller nanospherical SOMs formed from $[Mo_{72}Fe_{30}]$. After an interval of 1 h, the morphology of the particles in dispersion changes to nanodonuts [Fig. 1(c)]. We believe that $Mo_{72}Fe_{30}$ unit breaks down in dispersion due to the disruption by emergent SOM-peapod nanorods from $[PMo_{12}]$. Free Fe^{3+} ions are released in the dispersion which further help self-condensation of SOM-peapod nanorods which have MoO_3 units on their surface that condense via Fe^{3+} ions and finally form nanodonuts. To further prove that Fe^{3+} catalyzes the self-condensation of peapods, we added Fe^{3+} in the dispersion of peapods to test if we can induce the formation of nanodonut-type morphology of comparable length scales from peapods (Fig. 2). We found that the self-assembly between peapods indeed led to the formation of nanodonuts and on increasing Fe^{3+} ion concentration a net-type morphology (Fig. 2) not seen in the case of competitive self-assembly of our system. We thus in fact could induce different types of self-assemblies simply by variation of Fe^{3+} ion concentration in SOM-peapod system alone.

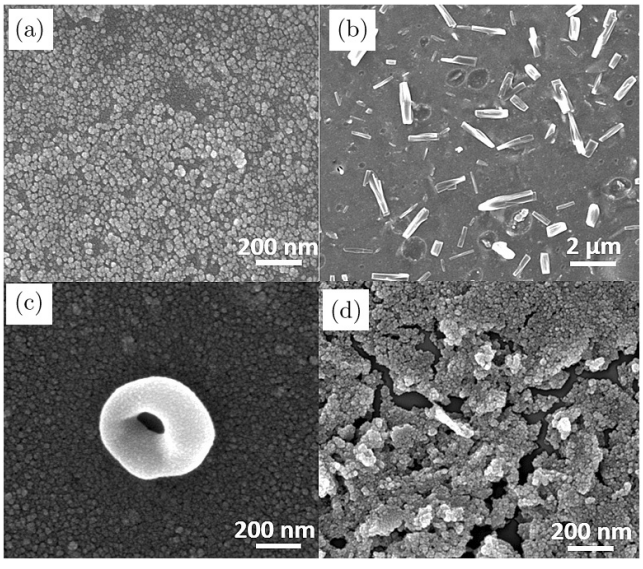

Fig. 1. SEM image of SD-SOM at different time intervals. (a) Initially after preparation of dispersion, (b) after 4 h, (c) after 5 h and (d) after 13 h from the preparation of dispersion.

In the present case, we observe that as very small fraction of clusters break into dispersion, the concentration of Fe^{3+} ions released from the clusters to dispersion is very small, thus we only observe

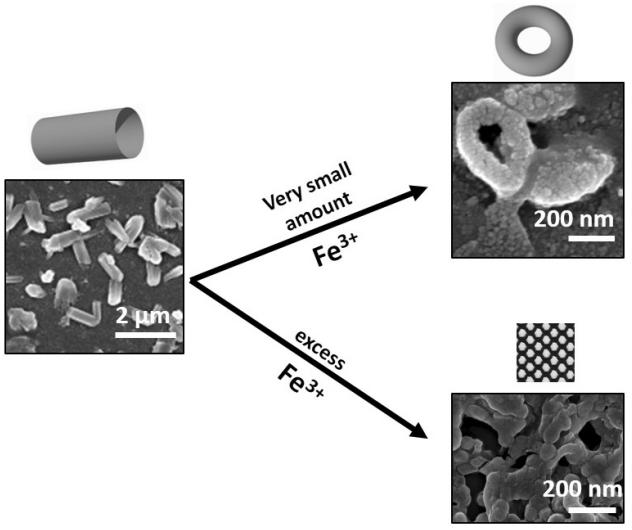

Fig. 2. Directed self-assembly of SOM-peapods with Fe^{3+} to nanodonuts and nets.

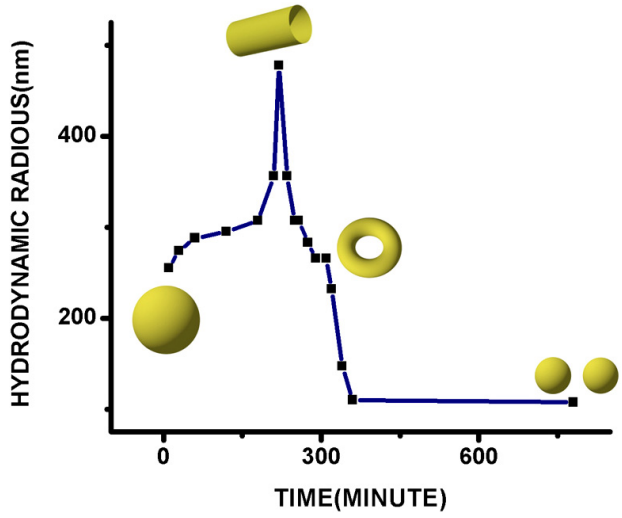

Fig. 3. Variation of hydrodynamic radius of SD-SOM with time.

nanodonuts morphology. At very small concentrations of Fe^{3+} ions, condensation of peapods to nanodonuts takes place whereas at higher concentrations of Fe^{3+} nanonets of peapods are formed. These nanodonuts further dissociate when kept for a long time finally giving nanospheres. Therefore in the experimental system in question, we finally obtained nanosphere morphology which are SOMs of non-disrupted $PMo_{12}O_{40}$ encapsulated $Mo_{72}Fe_{30}$ clusters [Fig. 1(d)]. Thus, in this present system we observe a clear time dependent topological transformation from nanosphere → nanorod → nanodonut → nanosphere, through the operation of a competitive size selective self-assembly pathway.

3.2. *Time dependent measurements of hydrodynamic radius of different morphology*

To show that we have a global phenomenon in the dispersion and not just a local microscopic phenomenon, we measured hydrodynamic radii of different morphological structures by dynamic light scattering (DLS). From the DLS experiments, it is observed that average size of the initial nanosphere i.e., $PMo_{12}O_{40}$ encapsulated $Mo_{72}Fe_{30}$ is around 255 nm, whereas the nanorod present in dispersion has an average hydrodynamic radius of 477 nm. This large size is attributed to the tumbling of the nanorods in dispersion, and it is due to this tumbling motion that the actual radius of nanorods cannot be obtained from DLS experiment. This average hydrodynamic radii values further prove that self-assembly takes place in dispersion at two different length scales. The average size of the particle when nanodonut is present in dispersion is found to be around 265 nm, and finally when SOMs of un-dissociated cluster are present in the dispersion i.e., small nanosphere has an average hydrodynamic radius of 110 nm. We have also performed time dependent DLS experiments to observe how hydrodynamic radii of the SOMs vary during this topological transformation by plotting hydrodynamic radii against time (Fig. 3). From the plot, it is observed that initially size increases with increasing time and reaches maxima when nanorods are present in dispersion, and hydrodynamic radii decreases rapidly with time and finally no variation is observed when undissociated clusters are present.

3.3. *Spectroscopic characterizations of topological transformation*

3.3.1. *Horizontal attenuated total reflectance infrared spectroscopy*

HATR-IR spectroscopy does not show any significant change during topological transformation, spectral pattern is found to be similar for different morphologies, and the similarity in spectral pattern may be attributed to the low number density of the different morphologies present in the dispersion in different time intervals. The spectrum shows four significant peaks at 2111, 1635 (δ_{O-H}), 1205 and a

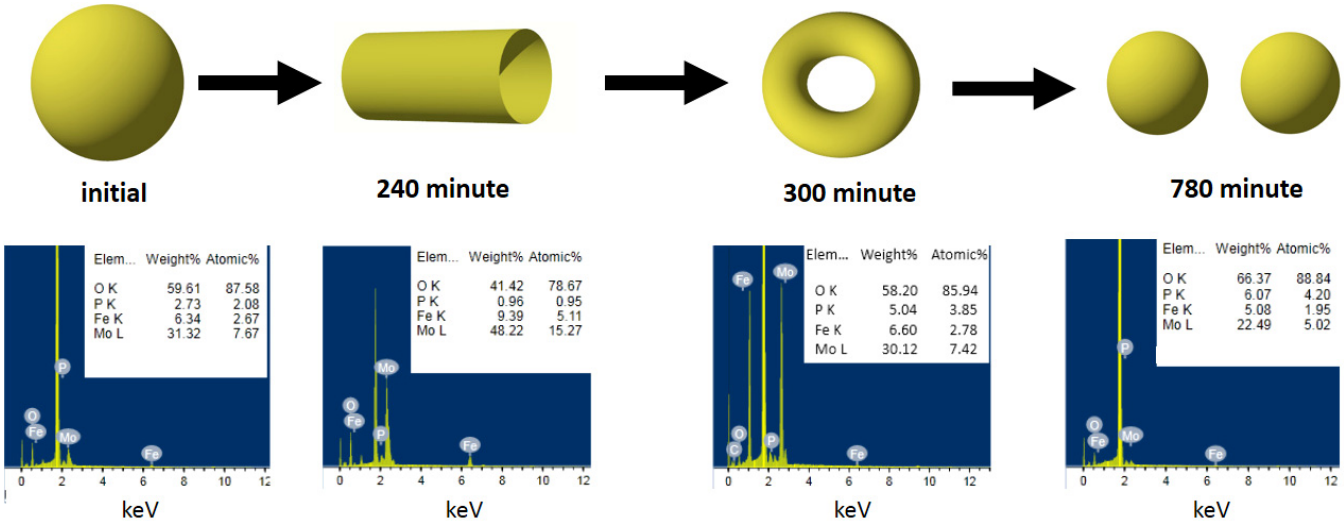

Fig. 4. EDS spectrum of different morphology at different time intervals.

broad peak at 695 ($\delta_{\mathrm{Fe-O-Mo}}$) cm^{-1} respectively for initially obtained nanosphere. After 4 h, when the topology has changed to nanorod, the spectrum shows five significant peaks at 2105, 1635 ($\delta_{\mathrm{O-H}}$), 1261, 691 ($\delta_{\mathrm{Fe-O-Mo}}$), 453 cm^{-1} respectively. After 5 h, it also shows five characteristic peaks at 2076, 1638 ($\delta_{\mathrm{O-H}}$), 1261, 724 ($\delta_{\mathrm{Fe-O-Mo}}$), 453 cm^{-1}, respectively when its topology is nanodonut, and after completion of topological transformation when it again comes back to nanosphere topology it shows four characteristics peaks at 2111, 1635 ($\delta_{\mathrm{O-H}}$), 1260 and a broad peak at 695 ($\delta_{\mathrm{Fe-O-Mo}}$) cm^{-1}. Here we observe a certain shift in the peak positions of the spectrum which suggests different bond strengths of the same bond in different morphologies which has different population of various vibrational levels (Fig. S1).

3.3.2. *Raman spectroscopy*

As the number density of the SOMs is very low we could not get proper Raman spectra for different topologies during the transformation. Instead we got some humps around 1250 cm^{-1}, 950 ($\gamma_{\mathrm{Mo=O}}$) cm^{-1}, 730 cm^{-1} respectively for all four different topologies implying the principal molecular component's (MoO_3) symmetry to be primarily invariant (Fig. S2).

3.3.3. *Molecular nature of competitive self-assembly of host–guest species*

Elemental analysis of the different topologies was obtained from the energy dispersive X-ray analysis (EDAX). From EDAX, it was observed that the atomic ratio of P:Fe:Mo was different for different morphologies (Fig. 4). This ratio for initial nanosphere is 1 : 1.28 : 3.69, for nanorod it was 1 : 5.38 : 16.07, 1 : 0.72 : 1.92 and for finally obtained small nanosphere the ratio is 1 : 0.46 : 1.19. Thus, we infer that atomic percentage of Fe and Mo first increases from nanospheres to nanorods, this may further be attributed to the disruption of hollow $Mo_{72}Fe_{30}$ spheres by peapods, as peapods have MoO_3 units therefore nanorods contained large amount of Molybdenum. Further condensation of peapod by Fe^{3+} leads to the formation of the ring which in turn decreases Molybdenum ratio in dispersion, and further this ratio gradually decreases

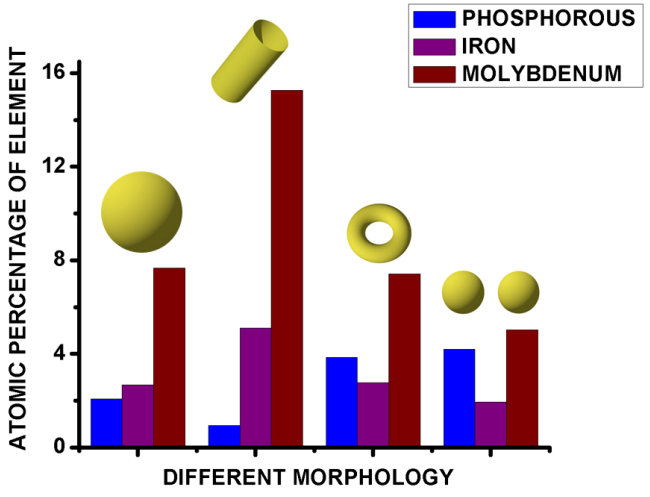

Fig. 5. Atomic percent of different elements in different morphologies.

from rod to donut to sphere (Fig. 5) validating an inference of the topological transformation.

4. Conclusion

In this paper, we present the operation of a size-selection rule dictated supramolecular Darwinism where a supramolecular host–guest complex of the type [PMo_{12}@$Mo_{72}Fe_{30}$] shows self-assembly of its components PMo_{12} and $Mo_{72}Fe_{30}$ in colloidal length scales as SOMs. We observe that larger species i.e., the nanorod dominates over the smaller size species i.e., nanosphere, and further condensation of those nanorods by Fe^{3+} ion leads to another morphology i.e., nanodonuts. These structures also dissipate with time. Finally, we obtain un-dissociated self-assembled nanospheres of [PMo_{12}@$Mo_{72}Fe_{30}$] which is nothing but undissipated SOMs of initial constituents. Here we present a clear topological transformation which takes place via competitive host–guest interaction. In the present case, following size-selection, larger species in the speciated system dominates over the smaller ones. The system in a way behaves similar to a Darwinian system and it is perhaps apt to say that Darwinism is manifested in the topological transformation of a precursor [PMo_{12}@$Mo_{72}Fe_{30}$] as it self-assembles to SOMs of larger length scales. Interesting oxometalate-based hybrid molecular and engineering can be structured following the procedure outlined in this work.

Acknowledgments

The authors thank DST-Fast track, BRNS-DAE and IISER-Kolkata for financial support.

References

1. T. Liu, *J. Am. Chem. Soc.* **125**, 312 (2003).
2. T. Liu, *J. Am. Chem. Soc.* **124**, 10942 (2002).
3. T. Liu, E. Diemann, H. Li, A. W. Dress and A. Müller, *Nature* **426**, 59 (2003).
4. A. Müller, E. Diemann, C. Kuhlmann, W. Eimer, C. Serain, T. Tak, A. Knöchel and P. K. Pranzas, *Chem. Commun.*, 1928 (2001).
5. A. Müller and C. Serain, *Accounts Chem. Res.* **33**, 2 (2000).
6. M. T. Pope, *Heteropoly and Isopoly Oxometalates* (Springer-Verlag, 1983).
7. A. P. Ginsberg, *Inorganic Syntheses* (John Wiley & Sons, 1990).
8. M. T. Pope and A. Müller, *Angew. Chem. Int. Edn. Engl.* **30**, 34 (1991).
9. D. L. Long, R. Tsunashima and L. Cronin, *Angew. Chem. Int. Edn.* **49**, 1736 (2010).
10. L. Cronin, *Angew. Chem. Int. Edn.* **45**, 3576 (2006).
11. T. Yamase and M. T. Pope, *Polyoxometalate Chemistry for Nano-Composite Design* (Springer Science & Business Media, 2002).
12. M. Pope and A. Müller, *Polyoxometalate Chemistry from Topology via Self-assembly to Applications* (Springer Science & Business Media, 2001).
13. U. Kortz, A. Mueller, J. van Slageren, J. Schnack, N. S. Dalal and M. Dressel, *Coord. Chem. Rev.* **253**, 2315 (2009).
14. M. A. AlDamen, J. M. Clemente-Juan, E. Coronado, C. Martí-Gastaldo and A. Gaita-Arino, *J. Am. Chem. Soc.* **130**, 8874 (2008).
15. X. Fang, T. M. Anderson, W. A. Neiwert and C. L. Hill, *Inorg. Chem.* **42**, 8600 (2003).
16. M. Bonchio, O. Bortolini, V. Conte and A. Sartorel, *Eur. J. Inorg. Chem.* **2003**, 699 (2003).
17. D.-L. Long, E. Burkholder and L. Cronin, *Chem. Soc. Rev.* **36**, 105 (2007).
18. D. L. Long, Y. F. Song, E. F. Wilson, P. Kögerler, S. X. Guo, A. M. Bond, J. S. Hargreaves and L. Cronin, *Angew. Chem. Int. Edn.* **47**, 4384 (2008).
19. J. Yan, J. Gao, D.-L. Long, H. N. Miras and L. Cronin, *J. Am. Chem. Soc.* **132**, 11410 (2010).
20. A. Müller, C. Beugholt, P. Kögerler, H. Bögge, S. Bud'ko and M. Luban, *Inorg. Chem.* **39**, 5176 (2000).
21. U. Kortz, F. Hussain and M. Reicke, *Angew. Chem. Int. Edn.* **44**, 3773 (2005).
22. L.-H. Bi, U. Kortz, M. H. Dickman, S. Nellutla, N. S. Dalal, B. Keita, L. Nadjo, M. Prinz and M. Neumann, *J. Cluster Sci.* **17**, 143 (2006).
23. C. P. Pradeep, D.-L. Long and L. Cronin, *Dalton Trans.* **39**, 9443 (2010).
24. C. Darwin, *Int. Sci. Library* (1859).
25. A. Müller, S. K. Das, H. Bögge, M. Schmidtmann, A. Botar and A. Patrut, *Chem. Commun.*, 657 (2001).
26. T. Liu, B. Imber, E. Diemann, G. Liu, K. Cokleski, H. Li, Z. Chen and A. Müller, *J. Am. Chem. Soc.* **128**, 15914 (2006).
27. G. Liu and T. Liu, *J. Am. Chem. Soc.* **127**, 6942 (2005).
28. G. Liu and T. Liu, *Langmuir* **21**, 2713 (2005).
29. D. Fan, X. Jia, P. Tang, J. Hao and T. Liu, *Angew. Chem.* **119**, 3406 (2007).
30. S. Roy, H. J. Meeldijk, A. V. Petukhov, M. Versluijs and F. Soulimani, *Dalton Trans.*, 2861 (2008).
31. A. A. Verhoeff, M. L. Kistler, A. Bhatt, J. Pigga, J. Groenewold, M. Klokkenburg, S. Veen, S. Roy,

T. Liu and W. K. Kegel, *Phys. Rev. Lett.* **99**, 066104 (2007).
32. T. Liu, M. L. Langston, D. Li, J. M. Pigga, C. Pichon, A. M. Todea and A. Müller, *Science* **331**, 1590 (2011).
33. S. Roy, L. C. Bossers, H. J. Meeldijk, B. W. Kuipers and W. K. Kegel, *Langmuir* **24**, 666 (2008).
34. A. Müller and S. Roy, *J. Mater. Chem.* **15**, 4673 (2005).
35. B. Roy, N. Ghosh, S. D. Gupta, P. K. Panigrahi, S. Roy and A. Banerjee, *Phys. Rev. A* **87**, 043823 (2013).
36. S. Roy, *Cryst. Eng. Commun.* **16**, 4667 (2014).
37. S. Roy, M. T. Rijneveld-Ockers, J. Groenewold, B. W. Kuipers, H. Meeldijk and W. K. Kegel, *Langmuir* **23**, 5292 (2007).
38. B. Roy, N. Ghosh, P. K. Panigrahi, A. Banerjee, A. Sahasrabudhe, B. Parasar and S. Roy, *J. Mol. Eng. Mater.* **2** (2014).
39. S. Roy, *Comments Inorg. Chem.* **32**, 113 (2011).
40. S. Roy, *Cryst. Eng. Commun.* **16**, 4667 (2014).
41. B. Roy, M. Arya, P. Thomas, J. K. Jürgschat, K. V. Rao, A. Banerjee, C. M. Reddy and S. Roy, *Langmuir* **29**, 14733 (2013).
42. S. Das, P. Thomas and S. Roy, *Eur. J. Inorg. Chem.* **2014**, 4551 (2014).
43. P. Thomas, C. Pei, B. Roy, S. Ghosh, S. Das, A. Banerjee, T. Ben, S. Qiu and S. Roy, *J. Mater. Chem. A* **3**, 1431 (2015).